

HYBRID MOTION CONTROL OF HUMANOID ROBOT FOR LEADER-FOLLOWER CO-OPERATIVE TASKS

by

Srdjan Ž. SAVIĆ*, **Mirko M. RAKOVIĆ***, **Branislav A. BOROVIĆ**,
and Milutin N. NIKOLIĆ

Faculty of Technical Sciences, University of Novi Sad, Novi Sad, Serbia

Original scientific paper
DOI:10.2298/TSCI151005037S

This paper presents a framework for leader-follower type co-operative transportation of an object by multiple humanoid robots or a single robot and a human. The emphasis in this paper is on the hybrid control algorithm and motion generation of the follower robot, while the influence of the leader has been simulated as external force acting on the follower's hands. The presented approach uses impedance controller to provide compliant behaviour of robot arms and it is an extension of our previous work on dual-mode impedance controller for safe human-robot interaction. Synthesis of the follower's legs and trunk motion is based on the reconfigurable adaptive motion primitives, which are defined as simple, parameterized motion building blocks that can be combined in a sequence or in parallel to generate complex motion. It has been already proven that motion generation, based on reconfigurable adaptive primitives enables the robot to modify gait parameters online, at any time instant, and synthesize dynamically balanced walk. Motion of the follower is based on the reactive approach, where the gait parameters (walking velocity, direction and step length) depend on intensity and direction of the external force vector. Robot end-effectors are compliant in horizontal plain, adapting to the physical guidance of the leader, while being stiff in vertical direction in order to compensate the external force in negative z-direction. The proposed framework has been tested by numerical simulations involving a dynamic robot model.

Key words: *co-operative transportation, impedance control, motion primitives, biped walking*

Introduction

Physical human-robot interaction (HRI) and co-operation has become a topic of increasing importance and major focus in robotics research [1] due to an existing tendency to incorporate robots and humans in a coexisting environment and to provide their cohabitation. A survey of robot interaction control schemes, based on static and dynamic model-based compensations was presented in [2], while a survey on robot-environment dynamic interaction, with a historical perspective on interaction control is given in [3]. One specific research topic within the HRI field is physical guiding of biped robots and wheeled mobile platforms in an unstructured environment. There are numerous applications where the robot and the human should move together, side by side, often maintaining physical contact during the mo-

* Corresponding author; e-mail: savics@uns.ac.rs

tion. Some possible applications include a caregiver guiding visually impaired persons or children.

Another, even more challenging research topic is the problem of co-operative transportation and carrying an object by multiple robots or the robot and the human. This task requires synchronized motion of all robots that participate in co-operative manipulation, as well as compliant behaviour which compensates for all the disturbances and model inaccuracies. As reported in [4], there are three main strategies for co-operation of multiple robots. The first strategy, which is also used in the control approach presented in this paper, is the leader-follower strategy. In this approach there is one master robot which does the path planning and imposes the desired motion while all the follower robots adapt and comply with this motion. The second strategy is the so-called leader-follower switch type where the robot which detects an obstacle, temporarily takes the role of the leader. The third strategy is a super leader strategy, where all the robots participating in the task are followers and the leader is the robot or the human outside the group, who provides the directives for the followers.

In this work, for motion control of the follower robot, arms impedance controller on a walking robot was used, and that is supposed to realize two tasks at the same time, *i. e.* walking and co-operative transportation, which is similar to scenario when two subjects (humans and/or robots) are carrying an object together. The synthesis of dynamically balanced walk is based on reconfigurable motion primitives (RAMP) [5-7]. The control of the robot's upper-body is based on impedance control in order to enable the compliant arms motion required during the execution of co-operative transportation of an object. The proposed framework consists of several modules: motion composition, dynamic balance control and joint motion control module. Motion composition module combines RAMP, simple motion building blocks, used for generation of complex motion of robot legs. Dynamic balance control module uses adaptive PID regulator to modify the values of desired angular velocities of legs and trunk, in order to preserve robot dynamic balance. Joint motion control module consists of two different non-linear controllers used for realization of reference joint motion. In order to provide compliance of the arms, joint-space impedance control was applied to robot arms. The main idea of the framework is to establish a relationship between external forces applied to robot's hands, measured with force sensors, and walking parameters. Relative displacement of the hands from the robot base segment and direction of the external force vectors are mapped to walking parameters that determine walking speed, direction and step length. The impedance controller is adopted in such a way to achieve lower impedance of the robot's end-effectors in the horizontal plain, thus complying with the physical guidance of the leader, while being stiff in the vertical direction in order to compensate for the weight of the object.

Related work

Several researches have been conducted on a mobile robot, force-guided by a human user, holding its hand. In [8] a joint-space impedance control approach was presented for a wheeled mobile platform IRL-1, with two arms, which reacts on user's pushing and pulling the end-effectors. Measured external forces, from direct physical contact, are mapped into motion commands. Another application, from the field of healthcare, is a robotic nursing assistant, which helps patients to get up from the bed [9]. This robotic assistant is guided through a hospital using direct physical interface, by applying external force on robot end-effector.

Physical HRI interface for guiding a biped NAO robot in a parent-child-like behaviour was presented in [10]. The presented approach is based on sensorless force control where

the applied external force is estimated by measuring motor current in the arms. Gait parameters are calculated based on the displacement of arm from its reference position. Basic position controller was used for robot arms, which is not inherently compliant. In [11] a follow-walking control method for WABIAN-RII robot was presented which consists of a pattern synthesis and a balance motion control. The follow motion of the lower limbs was realized by switching pattern technique, while the co-operative motion control method was used to calculate a compensatory motion of the trunk and waist to provide robot balance.

There are many ongoing researches in the field of multiple robot co-operation [12, 13, 14], but most of them focus on wheeled robots. Humanoid, biped robots have a greater potential, than wheeled robots, for locomotion in unstructured environment which can include stairs and other obstacles. However, biped robots often have a lower stability margin and they are more sensitive to external disturbances. A framework of co-operative object transportation of two HRP-2 humanoid robots, in the leader-follower method, was presented in [4]. The follower robot was programmed to follow the leader robot based on the force sensor information measured on its hands. External force stretches the arms and robot generates a walking pattern online in order to ease the interaction force and to recover the reference hands position. Another approach, based on machine learning, was used in [15] to tackle the problem of co-operative human robot transportation for the humanoid robot without force sensors. It is based on the data from accelerometers and pressure sensors. In the training phase, a statistical model of behaviour execution is learned that combines Gaussian process regression with a novel periodic kernel, and in the execution phase predictions from the statistical model are compared with stability parameters derived from current sensor readings. A learning method for correcting position shift in a transportation task was proposed in [16]. The learning of behaviour was performed in a simulation environment using Q-learning, in order to compensate for the position shift caused by both body swinging during movement and the shift in the centre of gravity, by transporting an object.

Dual model impedance controller for safe HRI

In our previous paper [17], a dual mode controller was proposed that enabled safe human robot interaction. First mode is a joint-space impedance control which provides accurate trajectory tracking, under the assumption that the dynamic model is known and the force measurement is provided. It is used for free motion and constrained motion during object manipulation where impedance controller parameters are chosen to provide good positioning accuracy in unconstrained directions and small contact forces in direction of contact. Second control mode is controlled gravity compensation [17, 18], used for operation in the close vicinity of humans or in direct physical contact with them, in order to provide safe human-robot interaction. The dynamics of a humanoid robot as a highly non-linear, coupled and multivariable system is described with the expression:

$$[\mathbf{H}]f''(\vec{q}) + [\mathbf{C}]f'(\vec{q}) + \vec{G} = \vec{\tau} + [\mathbf{J}]^T \vec{F}_{\text{ext}} \quad (1)$$

where $\vec{\tau}$ – is a vector of driving torques, \vec{q} – a vector of generalized co-ordinates, $[\mathbf{H}]$ – a symmetric, positive-definite inertia matrix, $[\mathbf{C}]$ – a matrix which describes influence of Coriolis and centrifugal forces, \vec{G} – a vector of torques caused by gravitational forces, $[\mathbf{J}]$ – a Jacobian matrix and \vec{F}_{ext} – a vector of external force, exerted by the environment on the robot's end effector. In the following text vector and matrix dependencies in the brackets will be omitted to simplify the notation.

Under the assumption of known dynamic model, feedback linearization has been used to choose an appropriate driving torque which cancel system non-linearities and reduces the original system to a system of double integrators:

$$\bar{\tau} = [H]\bar{a} + \bar{C} + \bar{G} - [J]^T \bar{F}_{\text{ext}} \quad (2)$$

where \bar{a} is the new control input, chosen to provide the desired dynamic relation between the contact force and displacement error. This control input is determined from the operational space impedance model, described with the following differential equation:

$$[H_m](f''(\bar{x}) - f''(\bar{x}_d)) + [D_m](f'(\bar{x}) - f'(\bar{x}_d)) + [K_m](\bar{x} - \bar{x}_d) = \bar{F}_{\text{ext}} \quad (3)$$

Matrices $[H_m]$, $[D_m]$, and $[K_m]$ are desired operational inertia, damping and stiffness, constant in the operational space, and \bar{x} and \bar{x}_d are the actual and desired end-effector positions, respectively. These matrices have to be Hurwitz matrices to provide the stability of the system and are chosen to be diagonal, which means that impedance is decoupled for each operational space direction. In order to exploit system redundancy, impedance model was mapped to the joint space. Under the assumption that manipulator velocities are small, Jacobian derivative can be neglected. In order to provide joint space impedance model following kinematic and static relations were used:

$$d\bar{x} = [J]d\bar{q}, \quad f'(\bar{x}) = [J]f'(\bar{q}), \quad f''(\bar{x}) \approx Jf''(\bar{q}), \quad \bar{\tau}_{\text{ext}} = [J]^T \bar{F}_{\text{ext}} \quad (4)$$

Considering the assumption from eq. (4), joint space impedance model is obtained in the following form:

$$[J]^T [H_m][J](f''(\bar{q}) - f''(\bar{q}_d)) + J^T D_m J(f'(\bar{q}) - f'(\bar{q}_d)) + J^T K_m J(\bar{q} - \bar{q}_d) = [J]^T \bar{F}_{\text{ext}} \quad (5)$$

Motion planning, used in simulation, is based on setting the desired target point in the workspace to which the robot hand is supposed to move rectilinear. The direction of the desired Tool Center Point (TCP) velocity vector is such that vector points towards the target position in each time instant. More details about the used trajectory generation method can be found in [19]. Once the profile of the desired operational space velocity \vec{v}_{ref} is known, it is necessary to determine the vector of desired joint velocities $f'(\bar{q}_d)$ as:

$$f'(\bar{q}_d) = [J]^\dagger \vec{v}_{\text{ref}} + ([I] - [J]^\dagger [J])f'(\bar{q}_h) \quad (6)$$

where $[J]^\dagger = [J]^T([J][J]^T)^{-1}$ is the right pseudo-inverse of the Jacobian matrix. Vector \vec{q}_h is projected into the null space of Jacobian and enables exploiting system redundancy to solve the additional constraint, which is avoiding joints mechanical limits. Vector \vec{q}_h can be chosen in the following way:

$$\vec{q}_h = k_0 \left(\frac{\partial \omega(\bar{q})}{\partial \bar{q}} \right)^T, \quad \omega(\bar{q}) = -\frac{1}{2n} \sum_{i=1}^n \left(\frac{\bar{q}_i - \bar{q}_i}{\bar{q}_{i\text{max}} - \bar{q}_{i\text{min}}} \right) \quad (7)$$

where $k_0 > 0$ is constant gain, and $\omega(\bar{q})$ is the secondary objective function which maximizes the distance from joint mechanical limits. Vectors $\vec{q}_{i\text{max}}$, $\vec{q}_{i\text{min}}$ and \bar{q}_i are maximum and minimum joint limits and middle values of the joint ranges, respectively [20]. Desired angular positions and accelerations are obtained by integrating and differentiating desired velocity, respectively. Vector of the joint displacement can be noted as $\vec{q} = \bar{q} - \bar{q}_d$.

Control input \vec{a} which provides the desired impedance model of interaction between the robot end-effector and its environment is calculated from eq. (5) as:

$$\vec{a} = f''(\vec{q}_d) + [J]^\dagger [H_m]^{-1} ([J]^\dagger)^T \left([J]^T [D_m][J]f'(\vec{q}) + [J]^T [K_m][J]\vec{q} + [J]^T \vec{F}_{ext} \right) \quad (8)$$

Elements of matrices $[H_m]$, $[D_m]$, and $[K_m]$ are appropriately chosen to provide small contact forces in the constrained direction. The final expression for the driving torque is obtained by substituting eq. (8) into eq. (2).

Controlled gravity compensation is a special case of impedance controller used to actively imitate the behaviour of the robot with pure gravity compensation. Due to a compliance of an impedance controller, user is able to move the robot arm through physical interaction. The idea is to take the current robot arm configuration, described with vector \vec{q} , as a desired position \vec{q}_d for the impedance controller in each time instant. Desired joint velocity and acceleration are zero, since the robot should keep its current configuration when there is no external force:

$$\vec{q}_d = \vec{q}, \quad f'(\vec{q}_d) = 0, \quad f''(\vec{q}_d) = 0 \quad (9)$$

Substituting eq. (9) into eq. (8) control input \vec{a} is obtained, which provides behaviour similar to pure gravity compensation:

$$\vec{a} = f''(\vec{q}_d) + [J]^\dagger [H_m]^{-1} ([J]^\dagger)^T \left([J]^T [D_m][J]f'(-\vec{q}) + [J]^T \vec{F}_{ext} \right) \quad (10)$$

Damping term on the right hand side of eq. (10) prevents position drift when the external force decreases to zero. Substituting eq. (10) into eq. (2) gives the final expression for the driving torque.

Performance of the dual-mode impedance controller was verified through a numerical simulation performed only for the 7 DOF robot arm, with a fixed trunk. In the first simulation robot was in contact with the environment and it wrote a square on a board, modelled as an elastic element with high stiffness. Stick diagram of the simulated contact task is shown in fig. 1.

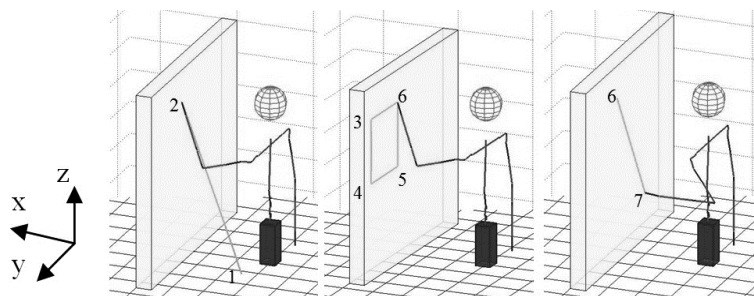


Figure 1. Stick diagrams of simulated arm movements: robot arm approaching the board (left); writing a square while in contact with the board (middle); robot arm detaching from the board (right)

Accurate trajectory tracking without overshoot was achieved in the unconstrained direction and robot successfully followed the desired square path in the Y-Z plane. Contact force was bounded in the constrained directions by decreasing the desired positioning accuracy. Friction between the robot arm and board was neglected. Hence, there was no contact

force in y and z-direction. Contact force in x direction depended on the board deformation, and it is shown in fig. 2.

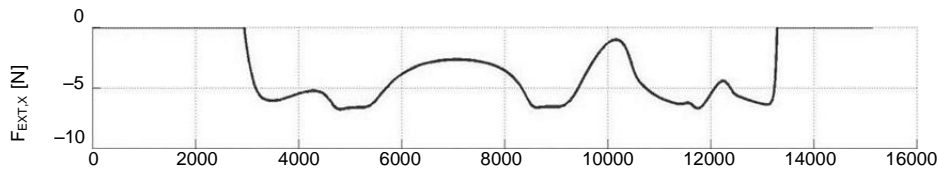


Figure 2. The X component of the contact force (normal to the board)

In the second simulation controlled gravity compensation mode of the controller was tested. Stick diagram of the simulated movement is shown in fig. 3. At the beginning of simulation robot arm was unconstrained, following the desired rectilinear trajectory using impedance control. At time intervals between 1-2 second and 4-5 second external forces F_{ext1} and F_{ext2} are applied on the robot hand in negative z-direction and robot controller switches to the controlled gravity compensation mode. In this phase, motion of the arm is driven by external force. After the external force decreases to zero, robot hand continuous to move towards the desired target point in the workspace.

Velocity and torque of the elbow joint are shown in fig. 3 and it can be noticed that, when external force decreases to zero, there is a short transient period where the damping term is decreasing the velocity to zero. So, the damping term prevents the joint from drifting, after the external force vanishes. In the presence of an external disturbance robot arm motion is compliant and driven by the external force while in the absence of the external force robot arm keeps the current position.

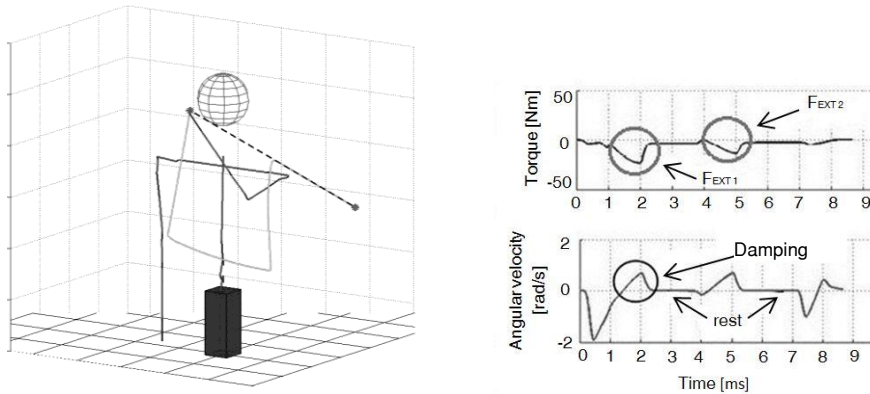


Figure 3. Stick diagram of robot motion in controlled gravity compensation mode (left); Graphic of angular velocity and torque for elbow joint (right)

The results presented in figs. 1-3 show that the use of impedance controller leads to accurate trajectory tracking in unconstrained directions while containing the contact force bounded. The performance of impedance controller is tested in controlled gravity compensation mode, which should be used when robot is in contact or in a close vicinity of a human. The results have shown that controlled gravity compensation provides safe and compliant behaviour, where the robot motion is driven by the action of external force. In the next chapter we will present the modified, *i. e.* extended version of dual mode impedance controller

integrated with RAMP based controller for walking. The goal is to achieve hybrid motion controller that is appropriate for walking humanoid robots during the execution of co-operative transportation tasks.

The RAMP-based framework for cooperative transportation

In paper [5] the developed RAMP-based controller was presented in details. It allows humanoid robot to synthesize and adapt its walking behaviour on-line with respect to the current state of the environment. Robot generates motion online by instantly changing its overall parameters of motion, which allows it to move efficiently in an unstructured environment. Walking pattern is completely described with four walking parameters: walking speed, walking direction, step length and the height to which the foot is lifted. The proposed RAMP-based controller consists of several modules: motion composition, dynamic balance control and joint motion control module.

Motion composition module takes as input values of four walking parameters, and combines motion primitives, as simple motion building blocks, to generate desired motion of robot legs. Each motion primitive has its own parameters which are related to walking parameters. If any of the walking parameters is changed, new primitive parameters are calculated instantly, and the desired motion is generated online to comply with the new walking parameters. The parameters can be changed at any time instant, during the motion execution, without stopping the execution of the current motion. The output from the motion composition block is the desired joint angular velocity vector, which corresponds to the desired walking parameters. However, the execution of the desired joint angular velocities fails to guarantee preservation of dynamic balance.

Dynamic balance controller is applied to introduce the corrections and calculate reference joint angular velocities. This control module uses adaptive PID regulator to modify the values of the desired angular velocities, in order to preserve robot dynamic balance. Modification is done on the basis of the distance between the desired and the actual values of zero moment point (ZMP) and projection of centre of mass (PCM), as well as of the current values of the joint angles and angular velocities. Two basic ideas behind this control approach are to avoid unpredicted serious endangerment of dynamic balance and to apply corrections smooth enough to keep the ZMP within the support area.

Joint motion control module consists of two different non-linear controllers. In our previous work sliding mode controller with disturbance estimator was used for realization of reference motion, calculated in the dynamic balance controller [5]. In this paper this control is used for lower limbs and robot trunk, but it is extended with a compliant controller for robot arms, necessary for co-operative manipulation task. Control algorithm for robot arms is based on joint-space impedance control, described in the section *Dual model impedance controller for safe HRI*.

The main idea of the framework is to establish a relationship between external forces applied to robot hands, measured with force sensors, and walking parameters.

Relative displacement of the hands from the robot base segment and direction of the external force vectors are mapped to walking parameters that determine walking velocity, direction and step length. Robot end-effectors are compliant in horizontal plain, adapting to the physical guidance of the leader, while being stiff in vertical direction in order to compensate for the weight of the object.

Overall model of the system dynamics, used in the simulation, includes robot dynamics model and dynamic model of actuators. Actuators in all actuated joints have been

modelled as DC motors with permanent magnets. Without loss of generality, it was assumed that all motors are the same. In order to express system dynamics in state space terminal inductance of DC motors was neglected on purpose. Dynamics of humanoid robot, with external forces and reaction forces from foot-ground contact, is represented by the following set of differential equations:

$$[H]f''(\bar{q}) + [C]f'(\bar{q}) + \bar{G} = \bar{\tau} + \underbrace{\sum_{i \in S_1} [J_i]^T \begin{bmatrix} \bar{F}_{\text{foot}i} \\ \delta_i \times \bar{F}_{\text{foot}i} \end{bmatrix}}_{\bar{\tau}_{\text{foot}}} + \underbrace{\sum_{i \in S_2} [J_i]^T \begin{bmatrix} \bar{F}_{\text{ext}i} \\ \bar{M}_{\text{ext}i} \end{bmatrix}}_{\bar{\tau}_{\text{ext}}} \quad (11)$$

where S_1 stands for indices of the points on the feet that are in contact with the ground, $\bar{F}_{\text{foot}i}$ and δ_i represent the force that appears at the i -th contact point and deformation of viscoelastic layer. Symbol S_2 stands for indices of the points where external forces are applied, $\bar{F}_{\text{ext}i}$ is the external force at i -th point, $\bar{M}_{\text{ext}i}$ – the vector of torque acting at i -th point, while $[J_i]$ represents the Jacobian calculated for the i -th contact point. Driving torques in robot joints are calculated based on mathematical model of DC motor given by the expression:

$$u_k = R_r i_{rk} + C_e f'(\bar{q}_k) + L_r f''(i_{rk}) \quad (12)$$

$$\bar{\tau}_k = C_m i_{rk} + B f'(\bar{q}_k) + J_r f''(\bar{q}_k) \quad (13)$$

where u_k represents the rotor voltage of the k -th motor, $\bar{\tau}_k$ is the driving torque at the joint k , i_{rk} – the rotor current of the k -th motor, $f'(\bar{q}_k)$ and $f''(\bar{q}_k)$ are the angular velocity and acceleration at the k -th joint, whereas terminal resistance R_r , terminal inductance L_r , speed constant C_e , torque constant C_m , torque/speed gradient B and rotor inertia J_r represent the motor parameters.

Overall model of the system dynamics in the state space in controllability canonical form is represented in the following form:

$$f'(\bar{x}_{ss}) = \begin{bmatrix} f'(\bar{q}) \\ \bar{f}(\bar{x}_{ss}) + \bar{g}(\bar{x}_{ss})\bar{u} + \bar{d} \end{bmatrix}, \quad f'(\bar{y}) = \bar{x}_{ss}, \quad \bar{x}_{ss} = \begin{bmatrix} \bar{q} \\ f'(\bar{q}) \end{bmatrix}, \quad f'(\bar{x}_{ss}) = \begin{bmatrix} f'(\bar{q}) \\ f''(\bar{q}) \end{bmatrix} \quad (14)$$

$$\begin{bmatrix} f'(\bar{q}) \\ f''(\bar{q}) \end{bmatrix} = \begin{bmatrix} f'(\bar{q}) \\ \underbrace{[\xi] \left(-[C]f'(\bar{q}) - \bar{G} + \bar{\tau}_{\text{foot}} - \frac{C_M C_e}{R_r} f'(\bar{q}) - B f''(\bar{q}) \right)}_{\bar{f}(\bar{x}_{ss})} + \underbrace{\frac{C_M}{R_r} [\xi] \bar{u}}_{\bar{g}(\bar{x}_{ss})} \end{bmatrix} + \underbrace{[\xi] \bar{\tau}_{\text{ext}}}_{\bar{d}}, \quad (15)$$

where $[\xi] = ([J_R][I] + [H])^{-1}$, \bar{x}_{ss} is the state vector, \bar{y} – the output vector (angular positions), \bar{q} – the vector of generalized co-ordinates, \bar{u} – the vector of motor voltages in each joint, $\bar{f}(\bar{x}_{ss})$ and $\bar{g}(\bar{x}_{ss})$ are non-linear state functions and $[I]$ is a unit matrix. Feedback linearization is used to calculate the appropriate control voltage \bar{u} :

$$\bar{u} = \bar{g}(\bar{x}_{ss})^{-1} (\bar{a} - \bar{f}(\bar{x}_{ss})) \quad (16)$$

Elements of the control input vector \bar{a} for the legs and the trunk joints are calculated as described in [5], based on sliding mode control with disturbance estimator. Those elements of the control input vector, related to upper limbs are calculated from the desired joint-space impedance model eq. (8), in order to provide compliant behaviour of robot arms. It

is assumed that the robot already holds the object at the beginning of simulation, and the arms are in a position suitable for carrying. Desired operational space linear velocity for robot hands is calculated with proportional-derivative (PD) controller, based on the displacement of the robot hand. If the external force displaces robot arm from its initial position, due to its compliance, PD controller generates desired velocity vector which leads the robot hand back to its initial position. Referent hand velocity is given with the following expression:

$$\vec{v}_{ref} = K_p \vec{x}_{err}(t) + K_D f'(\vec{x}_{err}(t)) \quad (17)$$

$$\vec{x}_{err}(t) = \vec{x}_d(t) - \vec{x}(t), \quad \vec{x}_d = \vec{x}_{init_dist} + \vec{r}_{base}(t), \quad \vec{x}_{init_dist} = \vec{x}_d(t_0) - \vec{r}_{base}(t_0) \quad (18)$$

where K_p and K_D are proportional and differential gain and $\vec{r}_{base}(t)$ is the position vector of base segment. Once the desired operational space velocity is determined, desired joint space velocity vector is calculated from eq. (6), where the secondary optimization objective, realized in the null-space of $[J]$, is to keep the initial configuration of the robot arm. Walking parameters are calculated on the basis of the measured external force applied to robot hand. Nominal value for all walking parameters is 1, except for direction which is 0. Walking direction is related to the angle between the external force vector and the unit vector of global coordinate frame x-axis. The current value for walking direction is gradually increased or decreased, in fixed discrete steps, to achieve the reference direction. The reference value is calculated from the following expression:

$$walk_dir = \arctg\left(\frac{F_{ext,y}}{F_{ext,x}}\right) \quad (19)$$

The values for walking speed and step length are proportional to each other, and they are related with the intensity of external force vector. These parameters are calculated from the following equations:

$$walk_speed = step_length = 1 + \frac{\text{sat}\left(\sqrt{(F_{ext,x})^2 + (F_{ext,y})^2}\right)}{20}; \quad \text{sat}(x) = \begin{cases} x, & \text{if } x \leq 5 \\ 5, & \text{if } x > 5 \end{cases} \quad (20)$$

Walking height parameter is irrelevant for the simulated task, and it was assumed to be constant with the nominal value 1.

Simulation results

Humanoid robot model described in [5] was used for simulation experiments. Software used for modelling and simulation of the robot has the capability of forming a dynamic model composed of a set of opened and closed kinematic chains. The model used in this paper has four kinematic chains and 51° of freedom. The contact between the foot and the ground is determined by six characteristic points (four contact points are at the corners of the foot body sole, and two are at the corners of the toe). In order to include the effects arising at the moment of establishing/breaking the foot-ground contact, the foot was defined as a rigid body with a viscoelastic layer on the sole that was modelled as an isotropic Kelvin-Voigt material.

The described humanoid robot model is used to conduct simulation experiments. In figs. 4-6, the stick diagram of the robot, footprints, the trajectories of ZMP position and the projection of the centre of mass are shown. In fig. 4 the simulation is shown when the robot was pulled by the external force applied on the left arm and at that time instant the walking

started. The applied force changes through time in the following order. From 0 to 6.6 second (during first two half steps) the force intensity is $[5 \ 0 \ -10]^T$, from 6.6 second to 16 second (during following three half steps) the force is $[3 \ 0 \ -10]^T$, and from 16 second to 22 second (during last two half steps) the force is $[1 \ 0 \ -10]^T$. During the walking, robot modifies online its step lengths and walking speed, with respect to the intensity of the applied force. From fig. 4. it can be seen that step length changes as the intensity of external force changes. During first two half steps, the half step length is the longest (around 50 cm), and in the case when the intensity of external force is lower, the robot online modify its step length and during the last two half steps, when the intensity of external force is lowest, the half-step length is around 42 cm.

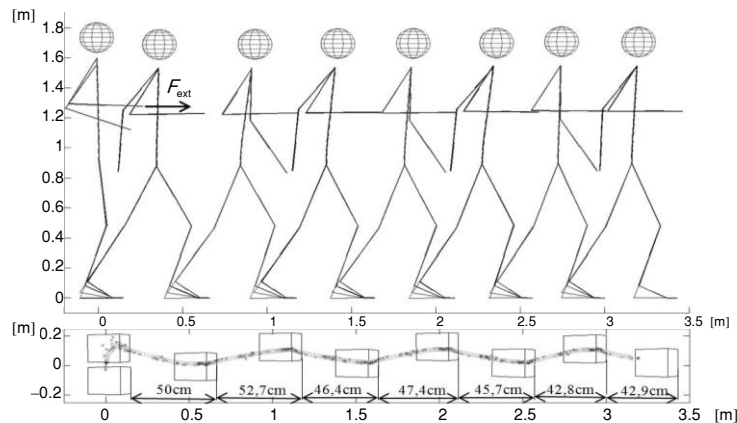


Figure 4. Stick diagram of the robot, positions of the feet, and the trajectories of ZMP (black crosses) and PCM (gray circles) during walking when the robot was pulled by the non-constant force

In figs. 5 and 6 the robot was pulled by external force that changes its direction through time in x-y plane in the following order. From 0 to 6.6 second the force is $[5 \ 0 \ -10]^T$ and afterwards the applied external force is $[4 \ 3 \ -10]^T$. Due to the change in direction of the external force, robot modifies its walking direction simultaneously with modification of the step lengths and walking speed, to comply with the direction and intensity of external force.

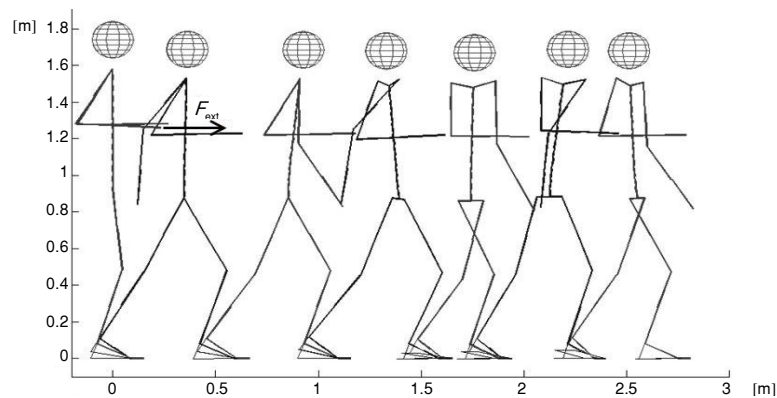


Figure 5. Stick diagram of the robot during walking when the robot was pulled by the force with the changing direction

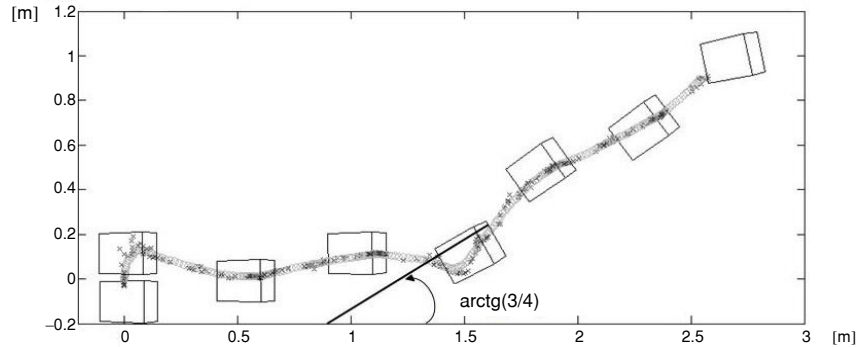


Figure 6. Positions of the feet, and the trajectories of ZMP (black crosses) and PCM (gray circles) during walking when the robot was pulled by the force with the changing direction

Conclusion

In this paper a framework of co-operative transportation by multiple humanoid robots was presented. The proposed framework is an extension of the previously presented dual-mode impedance control algorithm for compliant motion of robot arms, and a system for synthesis dynamically balanced walk based on reconfigurable adaptive motion primitives. Design of the control algorithm for the follower robot was emphasized in this paper, while the influence of the leader robot was simulated as external force acting on the follower's end-effector. Motion of the follower robot is induced as a reaction to the applied external force. Robot moves in the direction of the applied force with a velocity and step length proportional to the displacement of robot hands from their reference position. This way, the follower robot tends to ease the interaction force by walking. It was verified by numerical simulations that the proposed framework provides a robot with the ability to synthesize a dynamically balanced walk, guided by an external force, and to adapt it online to comply with the leader's motion. The future work will include a simulation of a leader-follower cooperative transportation in unstructured environment with dynamic obstacles, considering dynamics of both leader and follower robot, as well as dynamics of the carried object. Cooperative carrying by two humanoid robots, during stair ascending and descending will be also addressed.

Acknowledgement

This work was funded by the Ministry of Education, Science and Technological Development of the Republic of Serbia under contract III44008 and by Provincial Secretariat for Science and Technological Development under contract 114-451-2116/2011.

Nomenclature

\vec{a}	– control input, [rads ⁻²]	\vec{G}	– vector gravitational torques, [Nm]
B	– torque/speed gradient, [rpm/mNm]	[H]	– inertia matrix, [kgm ²]
[C]	– matrix of Coriolis and centrifugal forces, [kg m ² s ⁻¹]	[H _m]	– desired inertia matrix, [kgm ²]
C _e	– speed constant, [rpmV ⁻¹]	i _{ik}	– rotor current of the k-th motor, [A]
C _m	– torque constant, [Nm A ⁻¹]	[J]	– Jacobian matrix, [–]
[D _m]	– desired damping matrix, [kgs ⁻¹]	J _r	– rotor inertia, [kgm ²]
\vec{F}_{exti}	– external force at i-th point, [N]	[K _m]	– desired stiffness matrix, [Nm ⁻¹]
\vec{F}_{footi}	– reaction force at i-th point, [N]	L _r	– terminal inductance, [H]
		M _{exti}	– external torque at i-th point, [Nm]

\vec{q}	– vector of joint positions, [rad]	\vec{x}_{ss}	– state vector, [–]
\vec{q}_d	– vector of desired joint positions [rad]	\vec{y}	– state space output vector, [–]
R_r	– terminal resistance, [Ω]	<i>Greek symbols</i>	
$\vec{r}_{base}(t)$	– position of the base segment, [m]	$\vec{\tau}$	– vector of driving torques, [Nm]
u_k	– rotor voltage of the k-th motor, [V]	$\vec{\tau}_{ext}$	– vector of external torques, [Nm]
\vec{v}_{ref}	– referent end-effector velocity, [ms^{-1}]	δ_i	– deformation of the viscoelastic layer at the i-th contact point, [m]
\vec{x}	– vector of the robot hand position [m]		
\vec{x}_d	– vector of the robot hand desired position, [m]		

References

- [1] Haddadin, S., *et al.*, Safe Physical Human-Robot Interaction: Measurements, Analysis & New Insights, in: *Robotics Research, Springer Tracts in Advanced Robotics* (Ed. M. Kaneko, Y. Nakamura), Springer Berlin Heidelberg, 2011, pp. 395-407
- [2] Chiaverini, S., *et al.*, A Survey of Robot Interaction Control Schemes with Experimental Comparison, *IEEE/ASME Transactions on Mechatronics*, 4 (1999), 3, pp. 273-285
- [3] Vukobratović, M., Robot-Environment Dynamic Interaction Survey and Future Trends, *Journal of Computer and Systems Sciences International*, 49 (2010), 2, pp. 329-342
- [4] Meng-Hung, W., *et al.*, Cooperative Object Transportation by Multiple Humanoid Robots, *Proceedings, IEEE/SICE International Symposium on System Integration (SII)*, Kyoto, Japan, 2011, pp. 779-784
- [5] Raković, M., *et al.*, Realization of Biped Walking in Unstructured Environment Using Motion Primitives, *IEEE Trans. Robot.*, 30 (2014), 6, pp. 1318-1332
- [6] Raković, M., *et al.*, Parameters Adaptation of Motion Primitives for Achieving More Efficient Humanoid Walk, *Proceedings, IEEE 12th International Symposium on Intelligent Systems and Informatics (SISY)*, Subotica, Serbia, 2014, pp. 233-237
- [7] Raković, M., *et al.*, Biped Walking on Irregular Terrain Using Motion Primitives, *Proceedings* (Ed. M. Ceccarelli, V. A. Glazunov), in: *Advances on Theory and Practice of Robots and Manipulators, Romansy 2014 XX CISM-IFTOMM Symposium on Theory and Practice of Robots and Manipulators*, Moscow, 2014, Vol. 22, pp. 265-273
- [8] Ferland, F., *et al.*, Taking Your Robot for a Walk: Force-Guiding a Mobile Robot Using Compliant Arms, *Proceedings, 8th ACM/IEEE International Conference on Human-Robot Interaction (HRI)*, Tokyo, Japan, 2013, pp. 309-316
- [9] Chena, T. L., Kemp, C. C., A Direct Physical Interface for Navigation and Positioning of a Robotic Nursing Assistant, *Advanced Robotics*, 25 (2011), 5, pp. 605-627
- [10] Dabrowski, J., *et al.*, Holding Hands – Guiding Humanoid Walking Using Sensorless Force Control, *Proceedings, The 23rd IEEE International Symposium on Robot and Human Interactive Communication RO-MAN*, Edinburgh, UK, 2014, pp. 180-185
- [11] Hun-Ok, L., *et al.*, Follow-Walking Motions of a Biped Humanoid Robot, *Proceedings, 2000 IEEE/RSJ International Conference on Intelligent Robots and Systems, 2000 (IROS 2000)*, Takamatsu, Japan, 2000, Vol. 2, pp. 1334-1339
- [12] Kume, Y., *et al.*, Decentralized Control of Multiple Mobile Robots Handling a Single Object in Coordination, *Proceedings, IEEE/RSJ International Conference on Intelligent Robots and Systems, Lausanne, Switzerland, 2002*, Vol. 3, pp. 2758-2763
- [13] Hirata, Y., *et al.*, Leader-Follower Type Motion Control Algorithm of Multiple Mobile Robots with Dual Manipulators for Handling a Single Object in Coordination, *Proceedings, International Conference on Intelligent Mechatronics and Automation*, Chengdu, China, 2004, pp. 362-367
- [14] Stuckler, J., Behnke, S., Following Human Guidance to Cooperatively Carry a Large Object, *Proceedings, 11th IEEE-RAS International Conference on Humanoid Robots (Humanoids)*, Bled, Slovenia, 2011, pp. 218-223
- [15] Berger, E., *et al.*, Inferring Guidance Information in Cooperative Human-Robot Tasks, *Proceedings, 13th IEEE-RAS International Conference on Humanoid Robots (Humanoids)*, Atlanta, Geo., USA, 2013, pp. 124-129
- [16] Inoue, Y., *et al.*, Cooperative Transportation by Humanoid Robots – Learning to Correct Positioning, *Proceedings, Hybrid Intelligent Systems (HIS2003)*, Melbourne, Australia, 2003, pp. 1124-1133
- [17] Savić, S., *et al.*, Dual-Mode Impedance Controller for Safe Human-Robot Interaction, *Proceedings, The 7th International Conference on Engineering and Technology ICET-2015*, Hat Yai, Songkhla, Thailand, 2015

- [18] Wrede, S., *et al.*, A User Study on Kinesthetic Teaching of Redundant Robots in Task and Configuration Space, *Journal of Human-Robot Interaction*, 2 (2013), 1, pp. 57-81
- [19] Savić, S., *et al.*, SVM Regression-Based Computed Torque Control of Humanoid Robot Reaching Task, *Proceedings*, 2nd International Conference on Electrical, Electronic and Computing Engineering IcETRAN 2014, Vrnjacka Banja, Serbia, 2014
- [20] Sciavicco, L., Siciliano, B., *Modelling and Control of Robot Manipulators*, Springer-Verlag, London, UK, 2005